ISSN 0006-3509, Biophysics, 2015, Vol. 60, No. 6, pp. 893–899. © Pleiades Publishing, Inc., 2015.
Original Russian Text © O.I. Volokh, M.E. Bozdaganyan, K.V. Shaitan, 2015, published in Biofizika, 2015, Vol. 60, No. 6, pp. 1077–1084.

MOLECULAR BIOPHYSICS

Assessment of the DNA-Binding Properties of Actinomycin and Its Derivatives by Molecular Dynamics Simulation

O. I. Volokh[a], M. E. Bozdaganyan[a, b], and K. V. Shaitan[a]

[a] *Department of Biology, Moscow State University, Moscow, 119234 Russia*
e-mail: olesyavolokh@gmail.com
[b] *Federal Research and Clinical Center of Specialized Health Care and Medical Technologies, Federal Medico-Biological Agency, Orekhovyi bulv. 28, Moscow, 115682 Russia*

Received December 12, 2014; in final form, September 8, 2015

Abstract—A molecular dynamics simulation was used to assess the effect on the elasticity of a DNA fragment and the efficiency of DNA binding for actinomycins (antibiotics that are used in chemotherapy for certain oncology diseases). Hydroxyl and amino groups that were introduced as substituents in the phenoxazine ring of actinomycin were tested for their effect on the dynamic behavior and stability of antibiotic–DNA complexes. The Young modulus was calculated for DNA, DNA–actinomycin, DNA–7-hydroxyactinomycin, and DNA–7-aminoactinomycin. The free energy of complexation with DNA was calculated for actinomycin and its two analogs. The substituents were assumed to structurally stabilize the DNA fragment via additional hydrogen bonding.

Keywords: actinomycin, 7-aminoactinomycin, 7-hydroxyactinomycin, molecular dynamics.
DOI: 10.1134/S0006350915060275

INTRODUCTION

Actinomycin is an antibiotic of a streptomycete origin that is produced by *Streptomyces antibioticus* [1]. Actinomycins intercalate between base pairs into unwound DNA regions, moving the nucleotides apart and deforming the double helix at high concentrations [2–5]. The ability to produce a complex with such a structure is due to the structure of the actinomycin molecule, which consists of a phenoxazine chromophore moiety (which is known as actinocin) and two cyclic pentapeptide chains. Deformation of the double helix by intercalating actinomycin changes the mechanical characteristics of the complex. According to their mechanism of biological action, actinomycins are classed with the agents that selectively inhibit nucleic-acid synthesis (RNA synthesis) via complexation with template DNA through deoxyguanine residues [1] (Fig. 1). Actinomycin hinders the RNA polymerase progress along template DNA, thus terminating RNA strand elongation. The antibiotic sterically inhibits the reaction without directly interacting with the enzyme. Actinomycins block the RNA polymerase function by competitively binding to template DNA, indicating that their affinity for DNA is far greater than that of the enzyme. Ribosomal RNA synthesis is especially sensitive to actinomycin, whose pharmacological activity is determined by this issue. At higher concentrations, actinomycin inhibits DNA polymerase and may facilitate single-strand DNA breaks.

The interactions of actinomycin D and 7-aminoactinomycin D with DNA have been studied by experimental and theoretical biophysical methods [6–19]. In particular, studies have focused on the intercalation of actinomycins into single- and double-stranded

Fig. 1. The complex of actinomycin and double-stranded DNA. The phenoxazine moiety intercalates between guanine–cytosine pairs, while the peptide rings are accommodated in the DNA minor groove, thus stabilizing the structure.

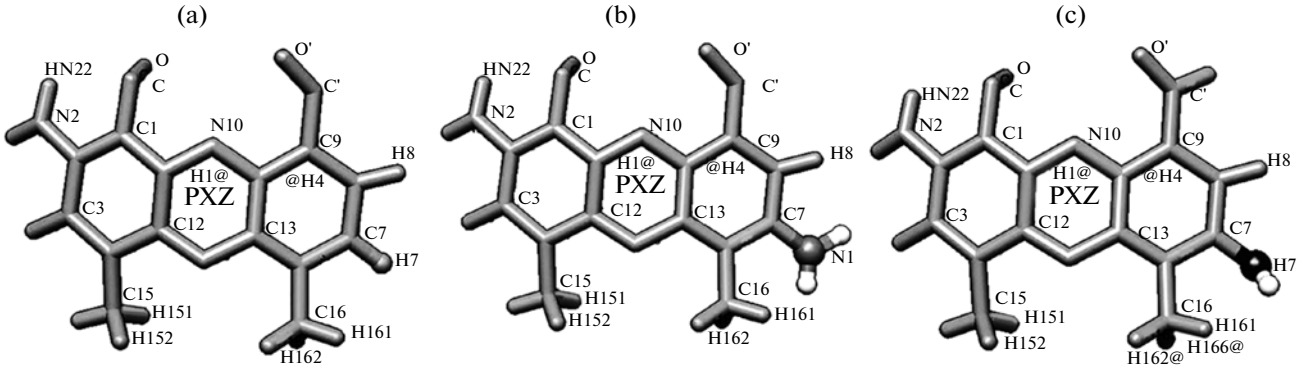

Fig. 2. The structures of actinomycin D and its analogs. (a) Original structure of the actinomycin fragment subject to modification. A substituent is introduced in position 7 of the phenoxazine chromophore ring. (b) Modified phenoxazine ring structure: an amino group is introduced in position 7. (c) Modified phenoxazine ring structure: a hydroxyl group is introduced in position 7.

DNAs, the melting of DNA–actinomycin clusters, the kinetics of intercalation into DNA, the spectroscopic properties of DNA–actinomycin complexes, and their photochemical activity. Substituents that were introduced in position 7 of the chromophore moiety have been shown to change the physico-chemical and biological properties of the complexes [7, 8]. The kinetics of actinomycin D intercalation in unwound DNA includes two phases, fast (seconds) and slow (minutes). Actinomycin D is weakly fixed within unwound regions, loops, and hairpin-like regions in the fast phase and enters the double helix in the slow phase [9]. X-ray analysis has shown that the methyl groups of the phenoxazine ring enter the DNA major groove and thereby anchor the antibiotic, while the amino group of the phenoxazine ring forms two hydrogen bonds with the DNA sugar-phosphate backbone [10, 11]. Circular dichroism and combinatorial light-scattering studies have demonstrated that the intercalation of actinomycins compared with other intercalating heterocycles dramatically changes the DNA structure, including regions outside the intercalation site [12–15]. Molecular dynamics (MD) simulations with actinomycin, 7-aminoactinomycin, and DNA fragment structures have shown that the structures are stable on 1-ns trajectories. DNA retains the B-DNA structure in these simulations, a slight bend forms in the antibiotic intercalation region, and nucleotide deviation from a parallel arrangement occurs in the phenoxazine moiety intercalation site [17]. Differential UV spectrophotometry and differential scanning microcalorimetry have revealed that DNA is stabilized in the intercalation sites and acquires a higher melting point and that actinomycin intercalates predominantly in satellite DNA, even at extremely low concentrations [5]. Intrinsic photochemical activity has been demonstrated for actinomycin D and 7-aminoactinomycin by spectroscopy, substantially facilitating the photodestruction of HeLa cells after entry by the antibiotics [6]. Using spectroscopy, the minimal energy of the actinomycin D–DNA fragment interaction has been estimated at approximately 3.7 kcal/mol [18]. Estimates that are similar in their order of magnitude have been obtained for the free energy of interaction ($\Delta G \sim 200$–500 kJ/mol) in a recent molecular dynamics study where the binding of DNA fragments with ligands has been analyzed by thermodynamic integration [19].

Actinomycin lacks selectivity and produces side effects, like many other antibiotics that are used in chemotherapy; it is therefore desirable to increase its affinity for DNA in order to reduce the dosage and administration frequency. We examined two actinomycin D analogs, 7-aminoactinomycin and 7-hydroxyactinomycin, because the relevant substituents are capable of additional hydrogen bonding to decrease the free energy without causing substantial structural alterations in the complex [1].

In this work, molecular dynamics was used to calculate the deformation free energy for the binding of actinomycin and its analogs 7-aminoactinomycin and 7-hydroxyactinomycin (Fig. 2) with DNA fragments; the objective was to evaluate the effects of the substituents that were introduced in the phenoxazine ring on the binding efficiency. The effect of complexation with actinomycin on the elasticity of the DNA fragment was evaluated by calculating the Young modulus for DNA complexes with actinomycin and its analogs.

METHODS

All of the numerical experiments were carried out with an AMBER force field [20] and the SPC-E classical three-center water model [21]. Trajectories were generated in the NPT ensemble at 300 K (the Parinello–Raman thermostat), with the Nose–Hoover barostat (isotropic pressure, all pressure components were 1 b). The Gromas 4.0.3 software package was employed in molecular dynamics [22]. The cutoff radius was 1.8 nm for the Lennard–Jones potential [23]; the particle mesh Ewald (PME) method [24] with a cutoff radius of 1.8 nm [23] was used to calcu-

Table 1. The computational system parameters for the task of evaluating the effect of actinomycins on the elasticity of a DNA fragment

System	Computational cell size, nm	Number of atoms	Number of counterions	Trajectory length, ns
DNA	5.7 × 8.7 × 5.7	6939	16	2.5
DNA + actinomycin	5.7 × 8.7 × 5.7	7115	16	2.5
DNA + 7-hydroxyactinomycin	5.7 × 8.7 × 5.7	7116	16	2.5
DNA + 7-aminoactinomycin	5.7 × 8.7 × 5.7	7118	15	2.5

Table 2. The computational system parameters for the task of evaluating the efficiency of actinomycin binding with DNA

System	Computational cell size, nm	Number of atoms	Number of counterions	Trajectory length, ns
Actinomycin	4 × 6 × 4	3128	0	50
DNA + actinomycin	4 × 6 × 4	3698	16	50
7-Aminoactinomycin	4 × 6 × 4	3131	0	50
DNA + 7-aminoactinomycin	4 × 6 × 4	3701	15	50
7-Hydroxyactinomycin	4 × 6 × 4	3129	0	50
DNA + 7-hydroxyactinomycin	4 × 6 × 4	3699	16	50

late the electrostatic interactions. The integration step was 1 fs; the trajectory length was no less than 1 ns. Charge calculations were performed with the GAMESS software package, using the 6-31GF basis with optimization of the molecule geometry. The trajectory length was 2.5 ns for calculating the Young modulus and 50 ns for calculating the free energy.

The computation systems are characterized for each task in Tables 1 and 2.

RESULTS

The effect of actinomycins on the elasticity of a DNA fragment. The effect actinomycins exert on the elasticity of a DNA fragment was evaluated by calculating the nucleic acid fragment stretch modulus and comparing the values that were obtained for the free DNA fragment and the corresponding DNA–antibiotic complexes. The stretch modulus was calculated as described for DNA fragments and DNA–ligand (nucleosome) complexes [25].

The DNA–actinomycin structure we examined had the ID of MNV [26] and the nucleotide sequence 5'-ATG|CTGCAT-3' where | is actinomycin. The structures of DNA complexes with the actinomycin analogs were obtained by modifying the original actinomycin molecule in the IMNV structure [26], using the Chimera program [27]. A crystal structure with this DNA sequence was chosen for further studies and modification because the lowest dissociation constant is characteristic of actinomycin complexes with the TGC nucleotide sequence [28, 29]. The resulting DNA–antibiotic structures were subjected to equilibrium molecular dynamics at 300 K for 500 ps to optimize the DNA structure after introducing the substituents in actinomycin because the amino and hydroxyl groups change the structural geometry.

To measure the elasticity modulus by nonequilibrium (steered) molecular dynamics, the upper pair of the bases DA5 and DT3 was fixed; fixation was performed at three coordinates. Acceleration was applied to the opposite end of the nucleic acid fragment. Accelerations were applied to the chain phosphorus atoms P8 and P11 (the last but one base pair because the terminal DA5 had no phosphate). The accelerations were 6, 8, and 10 nm/ps^2 along the coordinate y with both of the systems; the corresponding forces were 9, 12, and 15 kcal/(mol Å).

The Young modulus was calculated as $E = FL_0/(A_0\Delta L)$, where F is the force (newtons) applied to the strand end, A_0 is the area (A_2) where the force is applied, L_0 is the initial distance (nm) between the centers of mass of the terminal phosphorus atoms, and ΔL is the relative change (nm) in the distance.

Computations were performed in parallel for a DNA–antibiotic complex and the same DNA structure without the antibiotic in order to evaluate its effect on the strand elasticity. The Young modulus was calculated for the following structures: DNA, DNA–actinomycin, DNA–7-hydroxyactinomycin, and DNA–7-aminoactinomycin.

Figure 3 show the plots that were obtained for the distance between the centers of mass of the terminal phosphorus atoms in calculations performed for DNA–actinomycin, DNA–7-hydroxyactinomycin, DNA–7-aminoactionomycin, and DNA.

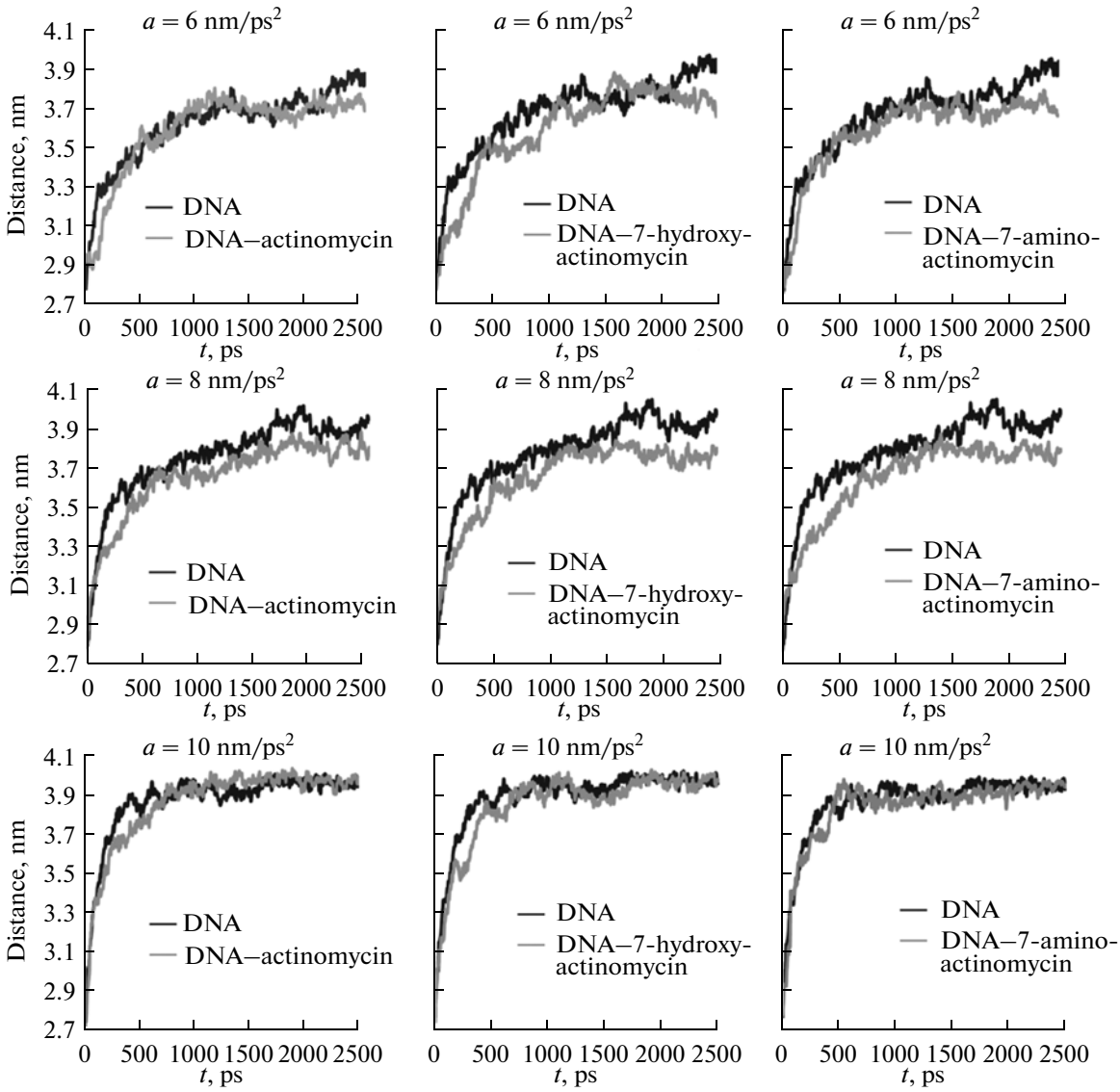

Fig. 3. The dependences of the distance between the centers of mass of the terminal pair phosphorus atoms at various accelerations as obtained for DNA and the DNA–actinomycin, DNA–7-hydroxyactinomycin, and DNA–7-aminoactinomycin complexes.

The Young modulus estimates that were obtained for DNA–actinomycin, DNA–7-hydroxyactinomycin, DNA–7-aminoactionomycin, and DNA are summarized in Table 3.

As is seen from the plots (Fig. 3), actinomycins affect the elasticity of the nucleic acid fragment at a time of approximately 1 ns (the nucleic acid in complex with the antibiotic stretches more slowly at the corresponding time points). A higher stiffness of the DNA–actinomycin complex is similarly evident from a higher Young modulus compared with that obtained for DNA without the antibiotic. However, differences in behavior between the structures became virtually undetectable after 1.5 ns. This might be caused by a

Table 3. Young modulus calculated for DNA and the DNA–actinomycin, DNA–7-hydroxyactinomycin, and DNA–7-aminoactinomycin complexes

Young modulus E, Pa			
DNA	DNA–actinomycin	DNA–7-hydroxyactinomycin	DNA–7-aminoactinomycin
1.0×10^9	1.9×10^9	2.4×10^9	2.6×10^9

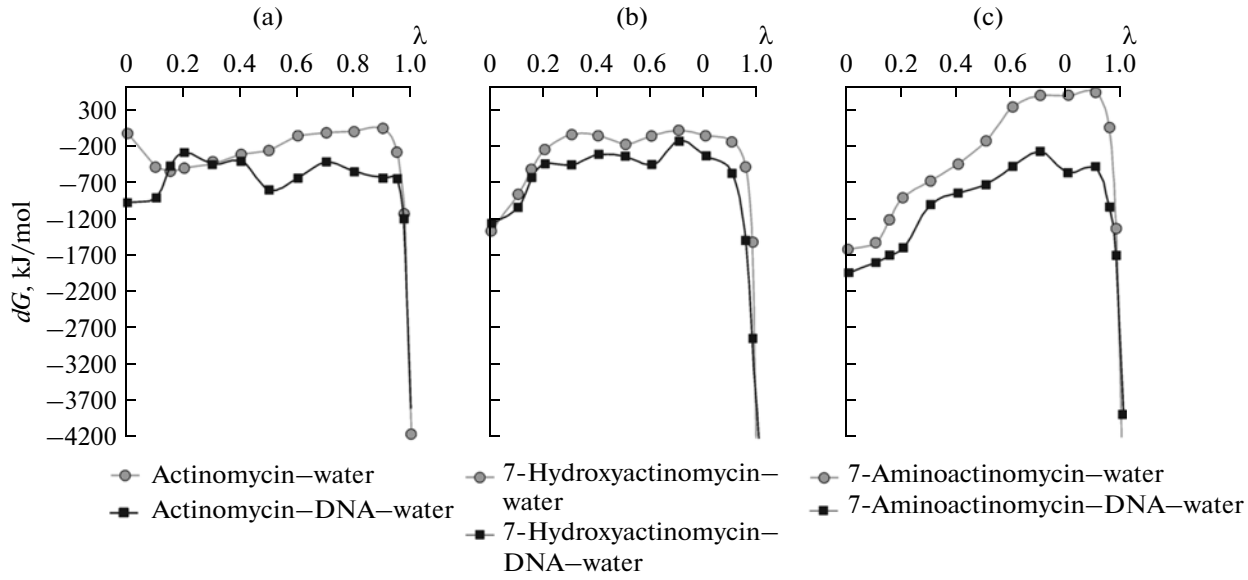

Fig. 4. The deformation free energies that were calculated for the DNA–antibiotic complexes. The λ dependence of $\partial G/\partial\lambda$ was obtained for various systems: (a) actinomycin–water and actinomycin–DNA–water, (b) 7-hydroxyactinomycin–water and 7-hydroxyactinomycin–water, and (c) 7-aminoactinomycin–water and 7-aminoactinomycin–water.

weaker stacking at greater distances between the nucleotide pairs where the antibiotic intercalates (the third and fourth pairs).

The following conclusion can be drawn from our findings. Actinomycin, 7-hydroxyactinomycin, and 7-aminoactinomycin increase the structural stiffness of the corresponding nucleic acid fragment, the increase is possibly due to a stacking of the phenoxazine moiety with parallel base pairs in the DNA strand. The result is supported by the higher Young modulus that is obtained for a stiffer structure, viz., a complex of the nucleic acid and the antibiotic 7-aminoactinomycin. In addition, a comparison of the plots that were obtained for different antibiotics demonstrates that 7-aminoactinomycin stabilizes DNA more efficiently than its analogs actinomycin and 7-hydroxyactinomycin. In order of the increasing Young modulus of the DNA fragment, the DNA–7-hydroxyactinomycin complex occupies an intermediate place between the DNA–actinomycin and DNA–7-aminoactinomycin complexes. A similar behavioral trend has been described for actinomycin complexes in the literature (see [2]).

The computational values were the same in their order of magnitude as experimental estimates [30–32] and correlated with published data [2], indicating that our molecular dynamics models of the DNA–antibiotic complexes are adequate and can be used for further research.

Efficiency of actinomycin binding with DNA. The input structures that are used to calculate the Gibbs free energy were the same as in calculations of the stretch modulus.

The deformation free energy was calculated by thermodynamic integration: $G^{B}(p, T) - G^{A}(p, T) = \int \partial H/\partial\lambda_{NpT} d\lambda$. Thermodynamic integration is one of the basic methods that is most commonly employed when estimating the free energy in molecular dynamics [24, 33–35].

The parameter λ, which influences the potential shape in the Hamiltonian, was varied incrementally from 0 to 1 (14 values were used: λ = 0, 0.1, 0.15, 0.2, 0.3, 0.4, 0.5, 0.6, 0.7, 0.8, 0.9, 0.95, 0.975, and 1.0). For each value of the parameter, molecular dynamics of the complexes was performed in water at 300 K for 2.5 ns. The energy was calculated at each step of the trajectory during simulation and the resulting values were averaged over time. Following the thermodynamic integration method [22], we computed two thermodynamic cycles, antibiotic–water (ΔG_1) and antibiotic–DNA–water (ΔG_2). The free energy of the antibiotic–DNA interaction was calculated as $\Delta G_{int} = \Delta G_2 - \Delta G_1$.

The energy that was calculated by this method is not equivalent to the free energy that is measured experimentally. The method makes it possible to calculate the energy for the "interaction" of two components of a system. A qualitatively adequate picture is obtained by comparing the computational values.

The λ dependences of $\partial H/\partial\lambda$ (an equivalent of the dependence of $\partial G/\partial\lambda$) that were obtained for each of the antibiotics by molecular dynamics simulation are shown in Fig. 4.

The deformation free energy estimates that were calculated for the antibiotic–DNA complexes (Table

Table 4. Deformation free energy calculated for antibiotic–DNA binding

Antibiotic	ΔG(antibiotic–H_2O), kJ/mol	ΔG(antibiotic–DNA–H_2O), kJ/mol	ΔG(antibiotic–DNA), kJ/mol
Actinomycin	−304 ± 0.1	−772 ± 0.1	−468 ± 0.2
7-Hydroxyactinomycin	−841 ± 0.1	−345 ± 0.1	−496 ± 0.2
7-Aminoactinomycin–water	−347 ± 0.1	−966 ± 0.1	−619 ± 0.2

4) were approximately 500 kJ/mol, suggesting a virtually irreversible binding to the DNA fragment for actinomycin and its derivatives.

The highest deformation free energy value was obtained for the nonmodified antibiotic: $\Delta G_{\text{actinomycin–DNA}} = -468 \pm 0.2$ kJ/mol. The second highest free energy was obtained for the hydroxyl-substituted actinomycin derivative: $\Delta G_{\text{7-hydroxyactinomycin–DNA}} = -496 \pm 0.2$ kJ/mol. The lowest value was observed in the case of the amino-substituted actinomycin derivative: $\Delta G_{\text{7-aminoactinomycin–DNA}} = -619 \pm 0.2$ kJ/mol. The mathematical error is included in the errors.

The results were used to estimate the contributions made by the substituents in position 7 of the phenoxazine moiety as compared with hydrogen in the same position (Table 5).

DISCUSSION

Actinomycin intercalation in a DNA fragment increased its stiffness in our experiments with DNA stretching. The computational experiments showed that the DNA fragment without the antibiotic stretched faster than the same structure with actinomycin or its analogs. The computational Young modulus estimates that was obtained for DNA agree well in their order of magnitude with the experimental data (about 10^9 Pa) [30–32]. The increase in DNA stiffness upon antibiotic binding supports the assumption that the structure is stabilized via the formation of additional bonds. A greater stabilization was observed with the amino-substituted antibiotic, possibly because the NH_2 group is capable of producing an additional hydrogen bond.

The results of the computational experiments show that the deformation free energy of 7-aminoactinomycin binding with DNA is substantially lower than in the case of the hydroxyl-substituted analog and nonmodified actinomycin. The greater contribution of the amino group compared with the hydroxyl group is most likely related to the number of additional hydrogen bonds. The results qualitatively correlate with experimental findings; i.e., the most efficient antibiotic–DNA binding has been reported for 7-aminoactinomycin [17].

Table 5. Energy contributions of the substituents introduced in position 7 of actinomycin

Contribution of the NH_2 group	−151 ± 0.4 kJ/mol
Contribution of the OH group	−28 ± 0.4 kJ/mol

Based on the results, a lower amount of antibiotic can be assumed to produce the same effect in the case of 7-aminoactinomycin compared with the hydroxyl-substituted analog or nonmodified actinomycin; i.e., toxicity and side effects might be lower. A qualitative picture is obtained with our method by estimating the deformation free energy of interactions because the energies of hydrogen bonds and dipole–dipole interactions are not calculated. However, thermodynamic integration makes it possible to reduce the simulation time, thus producing a qualitatively adequate picture.

ACKNOWLEDGMENTS

Computational experiments were performed using the Lomonosov supercomputer complex (Moscow State University). This work was supported by the Russian Science Foundation (project no. 14-14-00234).

REFERENCES

1. N. S. Egorov, *Fundamentals of the Science of Antibiotics,* 6th ed. (Moscow State Univ., Moscow, 2004) [in Russian].
2. Í. Sobell, Proc. Natl. Acad. Sci. U. S. A. **82**, 5328 (1985).
3. N. Vekshin and A. Kovalev, J. Biochem. **140**, 185 (2006).
4. J. Gill, M. Jotz, S. Young, et al., J. Histochem. Cytochem. **23** (11), 793 (1975).
5. N. Vekshin, J. Biochem. **149** (5), 601 (2011).
6. N. L. Vekshin, Biomed. Khim. **59** (3), 349 (2013).
7. N. S. Egorov, A. B. Silaev, and G. S. Katrukha, *Polypeptide Antibiotics* (Moscow State Univ., Moscow, 1987) [in Russian].
8. N. L. Vekshin, *Fluorescent Spectroscopy of Biopolymers (*Foton-Vek, Pushchino, 2008) [in Russian].
9. N. L. Vekshin and À. Å. Kovalev, J. Biochem. **140**, 185 (2006).
10. J. Meienhofer and E. Atherton, *Structure–Activity Relationship among the Semisynthetic Antibiotics*, Ed. by D. Perlman (Academic Press, New York, 1977), pp. 427–529.

11. E. F. Gale, E. Cunliffe, P. E. Reynolds, et al., *The Molecular Basis of Antibiotic Action* (Wiley, London, 1981).
12. L. Chinsky and P. Y. Turpin, Nucleic Acids Res. **5** (8), 2969 (1978).
13. M. Hou, H. Robinson, Y. G. Gao, and A. H. Wang, Nucleic Acids Res. **30** (22), 4910 (2002).
14. C. A. Frederick, G. J. Quigley, Ì. K. Teng, et al., Eur. J. Biochem. **181** (2), 295 (1989).
15. G. J. Quigley, A. H.-J. Wang, G. Ughetto, et al., Proc. Natl. Acad. Sci. U. S. A. **77**, 7204 (1980).
16. N. L. Vekshin, *Biphysics of DNA–Actinomycon Complexes* (Foton-Vek, Pushchino, 2009).
17. S. Ê. Sengupta, J. Å. Anderson, and C. Kelley, J. Med. Chem. **25**, 1214 (1982).
18. M. M. Khairetdinova and N. L. Vekshin, Russ. J. Bioorg. Chem. **40** (1), 56 (2014).
19. E. Marco, A. Negri, F. Gago, et al., Nucleic Acids Res. **33** (19), 6214 (2005).
20. Amber Tools Users Manual, http://ambermd.org/.
21. H. J. C. Berendsen, J. R. Grigera, and T. P. Straatsma, J. Phys. Chem. **91** (24), 6269 (1987).
22. *Gromacs Manual 4.0.3.*
23. M. Levitt, M. Hirshberg, R. Sharon, and V. Daggett, Comput. Phys. Comm. **91** (1–3), 215 (1995).
24. T. A. Darden and L. G. Pedersen, Environ. Health Perspect. **101**, 410 (1993).
25. A. Garai, S. Saurabh, Y. Lansac, and P. K. Maiti, J. Phys. Chem. B, **119** (34), 11146 (2015).
26. RCSB Protein Data Bank, www.rcsb.org.
27. UCSF Chimera Molecular Visualization Application, www.cgl.ucsf.edu/chimera.
28. H. M. Sobeli and S. C. Jain, J. Mol. Biol. **68**, 21 (1972).
29. J. Goodisman, R. Rehfuss, B. Wang, and J. C. Dabrowiak, Biochemistry **31**, 1046 (1992).
30. S. Cocco, J. Marco, and R. Monasson, C. R. Physique **3**, 569 (2002).
31. J. Marco and S. Cocco, Phys. World, No. 3, 37 (2003).
32. K. Bloom, Chromosoma, **117** (2), 103 (2008).
33. S. R. Varanasi, O. A. Guskova, A. John, and J.-U. Sommer, J. Chem. Phys. **142** (22), 224308 (2015).
34. N. Bieler and P. Hunenberger, J. Comp. Chem. **36** (22), 1686 (2015).
35. A. Y. Mehandzhiyski, E. Riccardi, T. S. van Erp, et al., J. Phys. Chem. B **119**, 10710 (2015).

Translated by T. Tkacheva

SPELL: 1. OK